Neurotoxicology and Teratology 100 (2023) 107304

Contents lists available at ScienceDirect

Neurotoxicology and Teratology

journal homepage: www.elsevier.com/locate/neutera

PFOS-induced dyslipidemia and impaired cholinergic neurotransmission in developing zebrafish: Insight into its mechanisms

Archisman Mahapatra [1], Priya Gupta [1], Anjali Suman, Shubhendu Shekhar Ray, Rahul Kumar Singh [*]

Molecular Endocrinology and Toxicology Laboratory (METLab), Department of Zoology, Banaras Hindu University, Varanasi, India

ARTICLE INFO

Editor: Dr. H Sable

Keywords:
Perfluorooctane sulfonate
Dyslipidemia
Cholinergic neurotoxicity
Zebrafish embryos
Gene expression

ABSTRACT

Perfluorooctane sulfonate (PFOS) is a persistent organic pollutant that has been widely detected in the environment and is known to accumulate in organisms, including humans. The study investigated dose-dependent mortality, hatching rates, malformations, lipid accumulation, lipid metabolism alterations, and impacts on cholinergic neurotransmission. Increasing PFOS concentration led to higher mortality, hindered hatching, and caused concentration-dependent malformations, indicating severe abnormalities in developing zebrafish. The results also demonstrated that PFOS exposure led to a significant increase in total lipids, triglycerides, total cholesterol, and LDL in a concentration-dependent manner, while HDL cholesterol levels were significantly decreased. Additionally, PFOS exposure led to a significant decrease in glucose levels. The study identified TGs, TCHO, and glucose as the most sensitive biomarkers in assessing lipid metabolism alterations. The study also revealed altered expression of genes involved in lipid metabolism, including upregulation of *fasn, acaca*, and *hmgcr* and downregulation of *ldlr*, *pparα*, and *abca1*, as well as decreased lipoprotein lipase (LPL) and increased fatty acid synthase (FAS) activity,suggesting an impact on fatty acid synthesis, cholesterol uptake, and lipid transport. Additionally, PFOS exposure led to impaired cholinergic neurotransmission, evidenced by a concentration-dependent inhibition of acetylcholinesterase activity, altered gene expressions related to neural development and function, and reduced Na^+/K^+-ATPase activity. STRING network analysis highlighted two distinct gene clusters related to lipid metabolism and cholinergic neurotransmission, with potential interactions through the pparα-creb1 pathway. Overall, this study provide important insights into the potential health risks associated with PFOS exposure, including dyslipidemia, cardiovascular disease, impaired glucose metabolism, and neurotoxicity. Further research is needed to fully elucidate the underlying mechanisms and potential long-term effects of PFOS exposure.

1. Introduction

Per- and Polyfluoroalkyl substances (PFAS) are emerging anthropogenic compounds characterized by their long carbon chain and extremely stable carbon-fluorine (C—F) covalent bond (Hallberg et al., 2019). With their exclusive characteristics of durability and hydrophobicity, PFAS are widely used in commercial and extensive industrial applications ranging from surfactants and lubricants to insulating agents and aqueous firefighting foams since 1950s (Zhang et al., 2016). This has attracted public attention due to their widespread distribution, persistent nature and adverse effects on wildlife and humans in the environment (Menger et al., 2020). They are resistant to degradation and have potential to bioaccumulate in food web. Therefore, they have been detected ubiquitously such as air, surface water, groundwater, sediments and food (Menger et al., 2020). Despite of legislation restricting their worldwide use in 2000, among all PFAS, PFOS in particular have arisen more concern in recent years due to its prevalent occurrence and increased concentrations in the environmental matrices including human populations and wildlife tissue (Jantzen et al., 2016).

PFOS ($C_8HF_{17}O_3S$) is a perfluorinated carboxylic acid (having hydrophobic alkyl chain and hydrophilic end group) surfactant and is extremely stable due to C—F bonds. PFOS has been predominantly

* Corresponding author.
E-mail addresses: amahapatra123@gmail.com, archisman@bhu.ac.in (A. Mahapatra), priyagupta78692@gmail.com, priya.gupta@bhu.ac.in (P. Gupta), rks.rna@gmail.com, rksrna@bhu.ac.in (R.K. Singh).
[1] Authors contributed equally.

https://doi.org/10.1016/j.ntt.2023.107304
Received 31 March 2023; Received in revised form 19 July 2023; Accepted 1 October 2023
Available online 5 October 2023

detected in blood samples of wildlife species, human and even in fetal cord blood also (ranging from pg/L to ng/ml) (Zheng et al., 2012). For instance, PFOS has been detected in fish samples, with 18 of the 23 target PFASs found in the fish samples. PFOS is the most predominant component, contributing 32.55% to the ∑PFASs in fish, likely arising from its bioaccumulation preference (Guo et al., 2023). PFOS has been detected in river water, with a study showing the use of electrochemical sensing to detect PFOS at sub-nanomolar levels in river water (Clark and Dick, 2020). Recently, the US Environmental Protection Agency (US EPA) in June 2022 have limited the PFAS usages and announced health advisory guidelines for restricting the use of PFAS, including limiting their concentration in drinking water under 20 pg/L (Cousins et al., 2022).

The accumulating studies have shown that PFOS causes multiple adverse effects such as immunotoxicity, hepatotoxicity, cardiovascular toxicity, reproductive toxicity, and endocrine disruption (Liang et al., 2022; Sun et al., 2018; Xu et al., 2022; Yin et al., 2021). Of particular interest, PFOS can interfere with lipid metabolism as evident from earlier studies on mice (Tan et al., 2012). Additionally, PFOS exposure can upset energy metabolism, particularly lipid metabolism, in zebrafish and other organisms, potentially leading to hepatic dysfunction (Mylroie et al., 2021). Besides this, PFOS toxicity studies also suggest potential neurotoxicity. For instance, lactational PFOS exposure in adult male mice showed alteration in hippocampus function and profound long-lasting effect in its behavior and learning patterns (Mshaty et al., 2020). Similarly, PFOS exhibited evident neurotoxicity and behavior defects after PFOS chronic exposure to *Caenorhabditis elegans* (Chen et al., 2014). However, limited evidence has pointed out the precise mechanism of action, more particularly in aquatic organisms.

Lipid metabolism is essential for brain development and function, as lipids are major components of neuronal membranes, myelin sheaths, and signaling molecules (Alecu and Bennett, 2019).. Alterations in lipid metabolism have been implicated in various neurodegenerative diseases, such as Alzheimer's disease and Parkinson's disease (Dai et al., 2021; Yan et al., 2022). However, the mechanisms by which lipid metabolism affects neuronal survival and function are not fully understood. PFOS is a persistent organic pollutant that has been shown to cause oxidative stress, apoptosis, and developmental toxicity in zebrafish embryos (Mahapatra et al., 2022; Shi et al., 2008). PFOS can also disrupt lipid homeostasis by affecting fatty acid synthesis, transport, and oxidation (Wan et al., 2012). However, the effects of PFOS on lipid metabolism and neurotoxicity in zebrafish embryos have not been explored.

The integrated biomarker response (IBR) index is a multivariate approach that integrate the multiple biomarkers into a unified parameter to assess the overall health status of organisms (Beliaeff and Burgeot, 2002). Notably, IBR is a useful tool in the assessment of toxicological endpoints, as it provides a comprehensive measure of the adverse effects of environmental toxins on biological systems and establish a “cause-result effect” between the toxicants concentration and biological response (Beliaeff and Burgeot, 2002).

Zebrafish (*Danio rerio*) have gained popularity as an outstanding in-vivo vertebrate model for ecotoxicology research with various advantages such as high degree of genetic and functional conservation with mammals, transparent body for in-vivo imaging, easy maintenance and a rapid development with optical clarity for high-throughput screening (Chia et al., 2022; Rea and Van Raay, 2020).Over the course of the past decade, zebrafish have increasingly been recognized as an important tool for investigating the multifaceted pathways and molecular mechanisms involved in lipid metabolism and neurotoxicity, providing insights that are highly relevant to human health.

The present study aimed to provide novel insights into the lipid metabolism and potential neurotoxic effects of PFOS exposure on zebrafish. The developmental effects, lipid parameters and the gene expression profiling of lipid metabolism were observed. In addition, we evaluated the multiple endpoints related to neurotoxicity, including AChE activity, touch-evoked behavior, and Na^+/K^+-ATPase activity. Moreover, the changes in gene expression of cholinergic neurotransmission were observed. Lastly, the potential risk of PFOS exposure to zebrafish was determined quantitatively by IBR. Taken together, these results will help to explore and understand the mechanism by which PFOS exposure alters lipid metabolism and neurotoxicity in zebrafish.

2. Material and methods

2.1. Zebrafish husbandry

Adult zebrafish (Tubingen strain, 6 months old) were procured from METLab, Department of Zoology, BHU (India). All zebrafish were acclimated in a semi-circulating water system and maintained under 14/10 h (light/dark) photoperiod cycle at 27 ± 5 °C (pH = 7.4–7.6, Salinity 0.1–0.2 ppt and Conductivity 300–600 μS). The fish were fed ad libitum with freshly hatched *Artemia nauplii* twice daily. Male and female adult zebrafish (2:1) were bred to collect embryos. All the fertilized embryos (blastocyst stage) were collected and staged under stereomicroscope for the subsequent experiment. All zebrafish husbandry and experimental protocols used for this study were compiled in accordance with the Animal Ethical guidelines and regulations set by the Institutional Animal Ethics and Care (IAEC), Banaras Hindu University, India (approval letter No. BHU/DoZ/IAEC/2019–20/020 Dated 27/08/2019).

2.2. PFOS exposure

At 4- h post-fertilization (hpf), zebrafish embryos were exposed at PFOS concentrations of 0.1 μM, 0.5 μM, and 1 μM (50 ppb, 250 ppb, and 500 ppb) prepared in E3 media. DMSO (0.05%) was used as vehicle control as PFOS stock solution was prepared in DMSO, this group is referred as 0 μM throughout the article. Approximately 10 eggs were chosen at random for each exposure group and kept in sterilized 12-well plates for 120 hpf at 27 ± 5 °C in a BOD incubator. About 80% of the exposure media was renewed daily after 24 h. Simultaneously, all the deceased embryos were discarded to maintain the exposure medium quality. Three biological replicates were conducted (n = 10) using fish from distinct breeding clutches collected over different weeks, and each biological replicate underwent three technical replicates with separate wells for each treatment group.

2.3. Embryo toxicity test

The OECD Test Guideline 236 for the fish embryo acute toxicity test was followed. Newly fertilized zebrafish eggs were exposed to the test chemical for 120 hpf and four apical endpoints were recorded as indicators of acute lethality in fish: (i) coagulation of fertilized eggs, (ii) lack of somite formation, (iii) lack of detachment of the tail-bud from the yolk sac, and (iv) lack of heart-beat. The mortality rate for each treatment group was calculated based on the number of embryos that showed any of these endpoints at 24 to 120 hpf. To observe the developmental abnormalities after 120 h PFOS exposure, embryos ($n = 6$) were imaged under stereomicroscope (Stemi 508, Zeiss). Developmental malformations such as yolk sac edema (YSE), pericardial edema (PE), body axis curvature and other obvious defects were recorded. The percent hatching was also calculated based on the number of hatched embryos out of total embryo. Malformation rate and morphology score was evaluated as mentioned earlier (Di Paola et al., 2022; Panzica-Kelly et al., 2010).

2.4. Study of lipid metabolism

2.4.1. Oil Red O (ORO) staining

Zebrafish embryos treated with PFOS exposure were processed for ORO staining. For this, the embryos ($n = 20$) were first fixed in 4% paraformaldehyde (PFA) for 24 h at 4 °C. Thereafter, the fixed embryos

were washed with PBS thrice for 10 min each. Then, the washed embryos were dipped with gradient of propylene glycol solution (from 20% to 100%) for 10 min each and stained with 0.5% ORO solution (in 60% isopropanol) for 4 h at room temperature (RT). The embryos were then washed with 60% isopropanol for 10 min following with PBS. The embryos were imaged using a stereomicroscope and a bright-field camera.

After imaging, the stained ORO was extracted from treated zebrafish embryos (n = 20) for the quantification analysis. PBS was withdrawn from each tube before adding 250 mL of 4% ethanol formed in 100% isopropanol. To ensure that the ORO stain was thoroughly removed, the samples were vortexed and then incubated overnight at RT. The extracted ORO stain solution was pipetted into corresponding 96-well plate and the OD (absorbance) was measured at 495 using multimode reader as described earlier (Al-Jamal et al., 2020).

2.4.2. Biochemical studies

At 96 hpf, 60 embryos were randomly chosen per group for enzyme sampling. The samples were homogenized in 10% phosphate-buffered solution (0.1 M). The homogenate then centrifuged at 2000 rpm for 20 min at 4 °C. After that, the supernatant was collected for biochemical parameters. The protein concentration was quantified following the Bradford method at 595 nm and standard graph was plotted using BSA as a standard (Bradford, 1976). Total lipid content was estimated using a Folch extraction method (Folch, 1941). Briefly, 1 mL of chloroform: methanol (2:1 *v*/v) was added to 100 μL of homogenized sample, mixed well and incubated at RT for 30 min. The mixture was then centrifuged at 10,000 *g* for 10 min, and the chloroform layer was collected for lipid estimation. The collected lipid fraction was evaporated, and the remaining lipids were weighed to determine the total lipid content. The levels of triglycerides (TG), total cholesterol (TCHO), LDL cholesterol, and HDL cholesterol in the homogenized samples were measured using commercially available enzymatic assay kits (Autospan). The sample was incubated with specific assay reagents that catalyzed the conversion of the lipid to a colored product, following the manufacturer's instructions for each lipid component. The absorbance of the product was measured at the wavelength specified by the kit, and the concentration of the lipid component was calculated using a standard curve prepared with known concentrations of the lipid. The glucose level in the homogenized samples was measured using a glucose oxidase-peroxidase method (Hill and Kessler, 1961). The sample was mixed with glucose oxidase and peroxidase enzymes, which oxidized glucose to gluconic acid and hydrogen peroxide, respectively. The H_2O_2 then reacted with a chromogen to produce a colored product. The mixture was incubated at 37 °C for 30 min to allow the reactions to complete. The absorbance of the product was measured at 540 nm, and the glucose concentration was calculated using a standard curve prepared with known concentrations of glucose.

2.4.3. Enzyme assays

After the exposure period, embryos (n = 50) were collected and homogenized in ice-cold homogenization buffer. The homogenate was centrifuged at 10,000 rpm for 10 min at 4 °C, and the supernatant was collected for enzyme assays. LPL and FAS enzyme activity was determined using a commercial assay kit according to the manufacturer's instructions (Abcam). The activities were expressed as units per milligram of protein.

2.4.4. Integrated biomarker response (IBR2)

The IBR2 was calculated using the formula described by Beliaeff and Burgeot (2002) and modified by Caliani et al. (2021). Briefly, the biomarker values were transformed to standard scores, and the average of the absolute values of the standard scores was used as the normalization factor. The normalized biomarker values were multiplied by their corresponding weight factors, and the sum of the weighted values was divided by the normalization factor to obtain the IBR2 value.

2.4.5. Gene expression analysis

Total RNA of treated and untreated zebrafish larvae (96 hpf) was extracted using TRIzol reagent (Ambion, Thermofisher) following the manufacturer's protocol. The purity (260/280) and quantity of extracted RNA was assessed using Eppendorf μCuvette® G1.0 bio spectrophotometer before proceeding further. Subsequently, total RNA was reverse-transcribed (RT) for cDNA preparation using cDNA Revert-Aid RT Transcription kit (Thermo Scientific™) in accordance with the manufacturer's instructions. Then, qRT-PCR was performed on QuantStudio 5 RT-PCR (Applied Biosystems) with reaction volume of 20 μl using SYBER Green qPCR Master mix (Thermo Scientific™, K0243). All analysis was carried out in triplicates. β-actin (house-keeping gene) was used as an internal standard. The function and primers for the genes (*fasn*, *acaca*, *hmgcra*, *ldlra*, *pparab*, *abca1a*, *lpla, manf, ache, ngfb, chata, slc18a3a, creb1a, bdnf*) used in this study are listed in Table S1 and S2 respectively. The 2-ΔΔCt technique was used to compute each gene's expression levels in Design and Analysis Software v1.5.2 (Applied Biosystems), which were then normalized against that of housekeeping genes (Livak and Schmittgen, 2001).

2.5. Assessment of cholinergic neurotoxicity

2.5.1. Acetylcholinesterase (AChE) enzymatic activity

After 96 hpf PFOS exposure, zebrafish larvae were taken randomly from each group for the determination of AChE activity. Briefly, the acetylcholine is hydrolyzed by AChE enzyme into choline and acetic acid, and further the obtained choline reacts to produce symtrinitrobenzene at 412 nm. For quantification, larvae (n = 30) were homogenized and centrifuged at 10000 rpm for 20 min at 4 °C. The obtained supernatant was then used for the estimation of AChE activity following Ellman et al. (1961). The specific activity of AChE was reported in U/mg protein.

2.5.2. Visualization of AChE activity

The activity of AChE in fixed zebrafish embryos was determined using the method described by Karnovsky and Roots (1964). Embryos at 24 hpf with a sample size of 10 were fixed overnight with 4% PFA. After fixation, the embryos were incubated in 60 mM sodium acetate buffer (5 mM sodium citrate, 4.7 mM $CuSO_4$, 0.5 mM $K_3(Fe(CN)_6)$, 1.7 mM acetylthiocholine iodide, pH 6.4) for 3–4 h and thoroughly washed with phosphate-buffered saline with Tween-20 (PBT) before observation under a Zeiss stereomicroscope (Stemi 508) connected to a Zeiss Axiocam 208 color digital camera.

2.5.3. Touch-evoked-escape behavior

To assess the touch-evoked escape (TEE) behavior, a random selection of ten embryos at 120 hpf was placed individually at the center of a plate (Ø 22 mm) containing E3 medium. Each embryo's tail was gently poked with a needle, and the distance traveled was captured by a video camera (60 frames per second) (Supplementary: Video_S1). We made a slight modification to the method described by Basnet et al. (2017) by adding an overlay of four concentric zones (Ø 5 mm = zone 1, Ø 10 mm = zone 2, Ø 15 mm = zone 3, and Ø 20 mm = zone 4) was added to each clip. We manually tabulated the embryo's location in response to the needle touch, based on the zone in which it ended up.

2.5.4. Na^+/K^+-ATPase activity

After 96 h PFOS exposure, the homogenized supernatant of zebrafish larvae was estimated using commercially available Na^+/K^+-ATPase enzymatic activity assay kit (Elabscience).

2.6. STRING network analysis

The STRING database (https://string-db.org/) was used to analyze the protein-protein interaction network of the proteins encoded by the genes whose expression levels were measured. The STRING database,

version 11.0, combines genomic context, high-throughput experiments, co-expression, and literature mining to predict functional associations between proteins. The interaction score was set to a medium confidence level of 0.4, which filters out interactions with a combined score lower than 400 in STRING. The protein network was visualized and clustered using the web-based viewer in STRING. The endpoints evaluated in the network analysis were the number of nodes, edges, clusters, and enrichment *p*-values for Gene Ontology terms and KEGG pathways.

2.7. Statistical analysis

The data obtained from the experiment was repeated three times and presented as mean ± standard deviation (SD). The data sets were analyzed using one-way ANOVA followed by Dunnett post hoc test. The graphs were created using GraphPad Prism software (version 9). The threshold for statistical significance was set at $P < 0.05$ for all experiments.

3. Results

3.1. Dose-dependent mortality and hatching rates of zebrafish embryos exposed to PFOS

The results of this study showed dose-dependent mortality of zebrafish embryos exposed to PFOS. The mortality (%) increased with increasing concentrations of PFOS at all time points examined, indicating the potential toxicity of PFOS to zebrafish embryonic development (Fig. 1A). The mortality (%) at 120 hpf was the highest among all time points, reaching up to 28.1% at the highest concentration of 1 μM. The mortality rates at earlier time points (24–72 hpf) were relatively lower than those at later time points (96–120 hpf).

The hatching rates of zebrafish embryos exposed to different concentrations of PFOS were assessed in this study, providing important insights into the potential developmental toxicity of this compound (Fig. 1B). Analysis of the data revealed that PFOS exposure had a concentration and time-dependent effect on the hatching (%) of zebrafish embryos. At 48 hpf, the hatching (%) of embryos exposed to 0.5 and 1 μM PFOS was lower compared to the control group, suggesting an early effect of PFOS exposure on embryonic development. At 72 and 96 hpf, exposure to higher concentrations of PFOS resulted in significant reductions in hatching (%), indicating a more pronounced effect on later stages of embryonic development.

3.2. PFOS impaired development

The present study investigated the developmental effects of PFOS on zebrafish embryos at 24, 48, 72, and 96 hpf. The malformation rate, defined as the percentage of malformed embryos out of the total embryos, was used as the endpoint for the current study. The results revealed that exposure to PFOS caused a concentration-dependent increase in the malformation rate in zebrafish embryos (Fig. 2A). At 24 hpf, the malformation rate was low across all PFOS concentrations tested. However, at 48 hpf, the malformation rate increased with increasing PFOS concentration, with the highest malformation rate observed at 1 μM PFOS. The trend continued at 72 hpf and 96 hpf, with the highest malformation rates observed at the highest PFOS concentration tested (1 μM). Analysis of the morphological scores (Table S3; based on which morphology scoring was done) revealed that at 1 μM concentration, the embryos exhibited severe malformations, with multiple abnormalities in their anatomical structures such as yolk sac edema, pericardial edema, body axis curvature, tail deformities etc. (Fig. 2B & Fig. 2C). At lower concentrations of 0.5 μM and 0.1 μM, the embryos exhibited moderate to mild malformations, respectively. However, even at these lower concentrations, the abnormal morphology observed in the embryos suggests the potential developmental toxicity of PFOS.

3.3. PFOS induced lipid accumulation

The ORO staining revealed a notable increase in lipid accumulation in PFOS-exposed zebrafish embryos compared to the control group (Fig. 3A). The intensity and extent of ORO staining appeared to be dependent on the dose of PFOS exposure, with higher doses resulting in more pronounced lipid accumulation. Vehicle Control embryos exhibited minimal ORO staining, indicating low levels of lipid accumulation.

The quantification analysis revealed a significant increase in

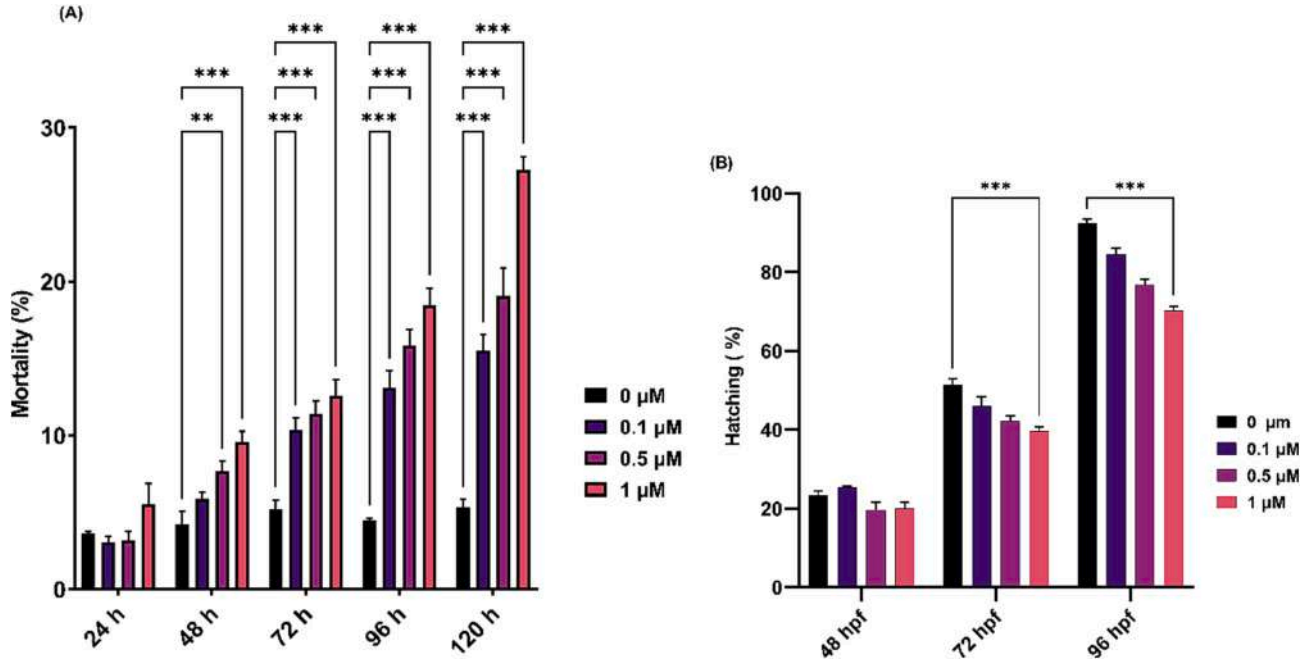

Fig. 1. The mortality (A) and hatching (B) of zebrafish embryos exposed to PFOS. Values represented as mean ± SD. Significance levels: $P < 0.05$, $P < 0.01$, and $P < 0.001$ denoted by *, **, and ***, respectively.

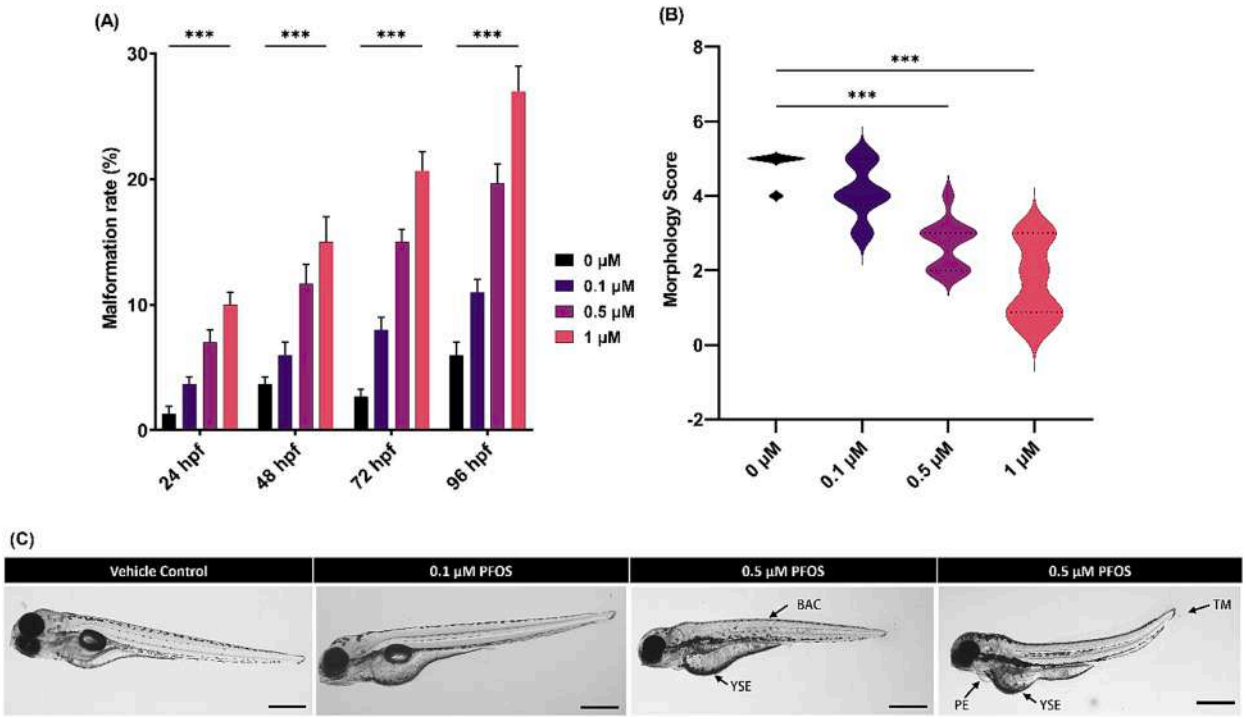

Fig. 2. (A) Malformation rate, (B) Morphology score and (C) Morphological changes observed in zebrafish larvae after 96-h exposure to different concentrations of PFOS (0 μM, 0.1 μM, 0.5 μM, and 1 μM). The morphological changes included body axis curvature (BAC), yolk sac edema (YSE), pericardial edema (PE), tail malformations (TM). Scale bar = 500 μm.

absorbance values in the PFOS-exposed embryos compared to the control group (Fig. 3B). The absorbance values correlated with the amount of extracted ORO stain, indicating higher lipid content in the PFOS-exposed embryos. Furthermore, the increase in absorbance was found to be dose-dependent, with higher PFOS concentrations leading to greater lipid accumulation.

3.4. PFOS exposure altered lipid contents

The study conducted at 96 hpf in zebrafish embryos exposed to different concentrations of PFOS revealed several noteworthy results. The data showed a significant increase in total lipid levels in embryos exposed to PFOS at concentrations of 0.5 μM and 1 μM compared to the control group (Fig. 4A). TGs (Fig. 4B) and TCHO (Fig. 4C) levels also increased in a dose-dependent manner, with the highest levels observed in embryos exposed to 1 μM PFOS. Similarly, LDL cholesterol levels showed a dose-dependent increase in embryos exposed to PFOS (Fig. 4D). Interestingly, HDL cholesterol levels decreased in embryos exposed to PFOS at concentrations of 0.1 μM and above, suggesting a possible adverse effect on lipid metabolism (Fig. 4E). Finally, glucose levels decreased in a dose-dependent manner in embryos exposed to PFOS, with the lowest levels observed in embryos exposed to 1 μM PFOS (Fig. 4F).

3.5. High IBRv2 index indicated most affected biomarkers

All biochemical indicators related to lipid metabolism demonstrated a statistically significant induction or inhibition in the exposure groups as shown in Fig. 5. The biomarker deviation index for TGs, TCHO and GLU (glucose) activity was larger than that of all other biomarkers, indicating that these three were the most sensitive biomarkers in this exposure study. IBRv2 values for 0.1, 0.5 and 1 μM were 117.02, 210.59 and 295.63, respectively, with very modest differences among groups (Fig. 5).

3.6. PFOS altered enzyme activities and gene expressions involved in lipid metabolism

The enzyme activity of LPL and FAS was assessed, along with the gene expressions of *fasn, acaca, hmgcra, ldlra, pparab, abca1a,* and *lpla*. The results showed a concentration-dependent decrease in LPL activity with increasing PFOS concentrations (Fig. 6A), while FAS activity exhibited an opposite trend, with increased activity at higher concentrations (Fig. 6B). Additionally, the gene expressions of *fasn*, *acaca*, and *hmgcra* were upregulated in a dose-dependent manner, indicating an increase in fatty acid synthesis in response to PFOS exposure (Fig. 6C). Conversely, *ldlra*, *pparab*, and *abca1a* gene expressions were downregulated in a concentration-dependent manner, suggesting decreased cholesterol uptake and transport (Fig. 6C). Interestingly, the expression of *lpla* exhibited a biphasic response, with a decrease at lower concentrations followed by an increase at higher concentrations as shown in Fig. 6C. Overall, these findings suggest that PFOS exposure alters lipid metabolism and gene expression in zebrafish embryos, potentially leading to adverse health effects. Further studies are warranted to elucidate the underlying mechanisms and implications of these changes.

3.7. PFOS impaired cholinergic neurotransmission

One of the main objectives of this study was to investigate the effects of PFOS exposure on the development and function of the nervous system in zebrafish embryos. To this end, a series of assays were performed to evaluate the behavioral, enzymatic, and molecular changes induced by PFOS in zebrafish larvae. The results revealed significant alterations in several parameters related to neurotoxicity and neurodevelopment.

3.7.1. Acetylcholinesterase activity

PFOS exposure resulted in a concentration-dependent inhibition of AChE activity in whole embryo homogenates, with the highest effect seen at 1 μM PFOS (Fig. 7A). This effect was confirmed by whole mount staining of 96 hpf larvae, which showed a clear decline in the AChE

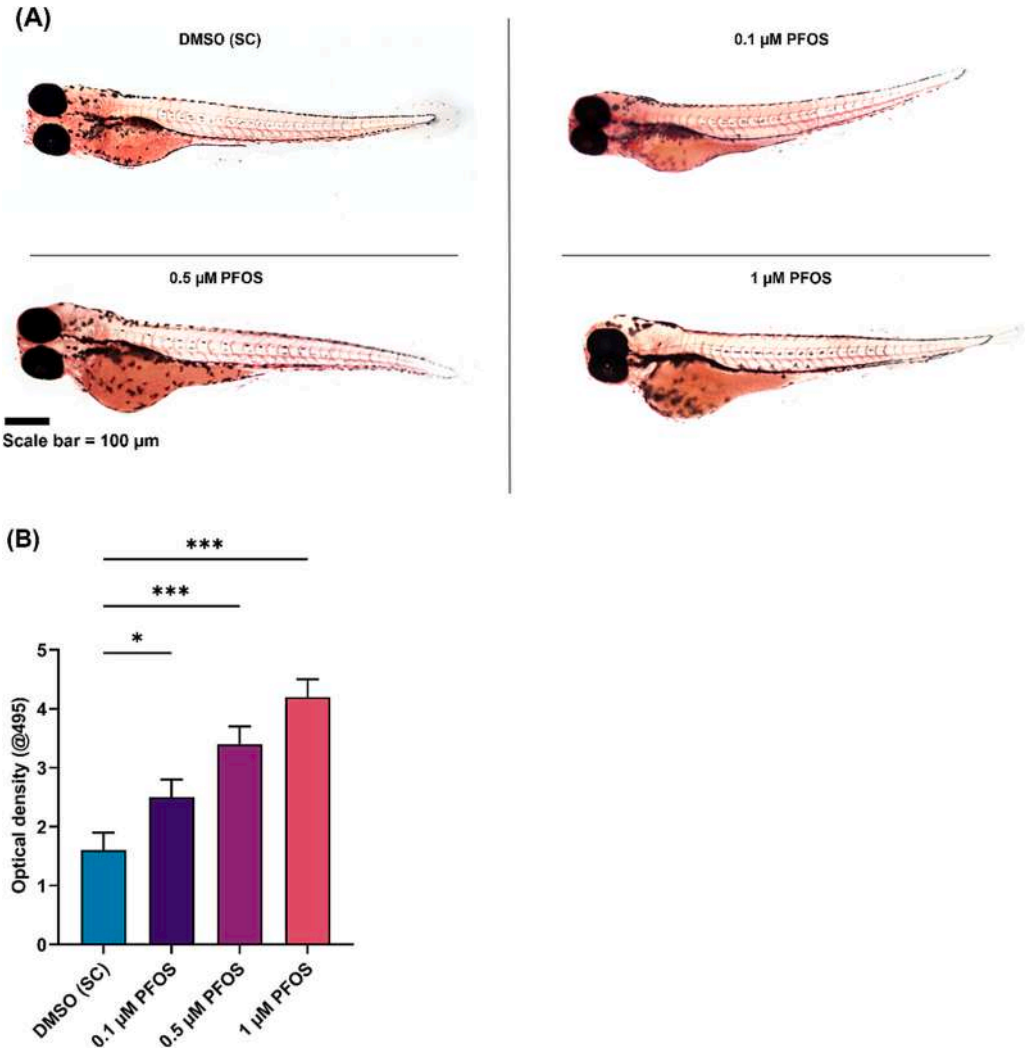

Fig. 3. (A) Representative images of ORO staining in zebrafish embryos exposed to different concentrations of PFOS. (B) Quantification analysis of ORO staining in PFOS-exposed zebrafish embryos. Values represented as mean ± SD. Significance levels: $P < 0.05$, $P < 0.01$, and $P < 0.001$ denoted by *, **, and ***, respectively.

activity in the trunk regions of embryo (Fig. 7B).

3.7.2. Touch-evoked escape behavior

The touch-evoked escape (TEE) behavior of 96 hpf larvae was assessed, which is a simple and reliable indicator of sensory-motor integration and neurological function. It was found that exposure to PFOS resulted in a significant reduction in the ability of larvae to respond to touch stimuli with increasing concentrations of PFOS, indicating impaired neurological function (Fig. 7D).

3.7.3. Gene expression of neural development and function factors

The mRNA levels of key genes involved in neural development and function were measured by quantitative real-time PCR (qRT-PCR). Genes that encode for neurotrophic factors (*manf, ngfb, bdnf*), enzymes related to cholinergic neurotransmission (*ache, chata, slc18a3a*), and transcription factors involved in neuronal plasticity (*creb1a*) were selected. It was found that exposure to PFOS resulted in alterations in gene expression of several factors, including *manf, ngfb, bdnf, ache, chata, slc18a3a*, and *creb1a* (Fig. 7E). The mRNA levels of *manf* and *ache* were upregulated in a concentration-dependent manner, suggesting compensatory responses to the observed AChE inhibition and neuronal stress. In contrast, the expressions of *ngfb, bdnf, chata, slc18a3a*, and *creb1a* were downregulated in a concentration-dependent manner.

3.7.4. Na^+/K^+-ATPase activity

Na^+/K^+-ATPase is essential for maintaining the resting membrane potential and regulating the excitability and signaling of neurons. PFOS exposure resulted in a significant inhibition of Na^+/K^+-ATPase activity in whole embryo homogenates in a concentration-dependent manner, with the highest effect observed at 0.1 μM PFOS (Fig. 7C).

3.8. STRING network analysis

To explore the possible interactions and pathways among the genes involved in lipid metabolism and cholinergic neurotransmission, we performed a string network analysis using the STRING database. The genes included in the analysis were related to lipid metabolism and cholinergic neurotransmission. The STRING network analysis showed that the genes formed two distinct clusters according to their biological functions (Fig. 8). The lipid metabolism cluster was composed of *fasn, acaca, hmgcr, ldlr, ppara, abca1,* and *lpl*, which are involved in fatty acid synthesis, cholesterol synthesis, lipoprotein uptake, lipid transport, and lipolysis. The cholinergic neurotransmission cluster was composed of *manf, ache, ngfb, chat, slc18a3, creb1,* and *bdnf,* which are involved in neuronal survival, acetylcholine hydrolysis and synthesis, acetylcholine transport, transcriptional regulation, and synaptic plasticity. However, the clusters were not completely isolated from each other and were found to be well connected via the *ppara-creb1* pathway (Fig. 8).

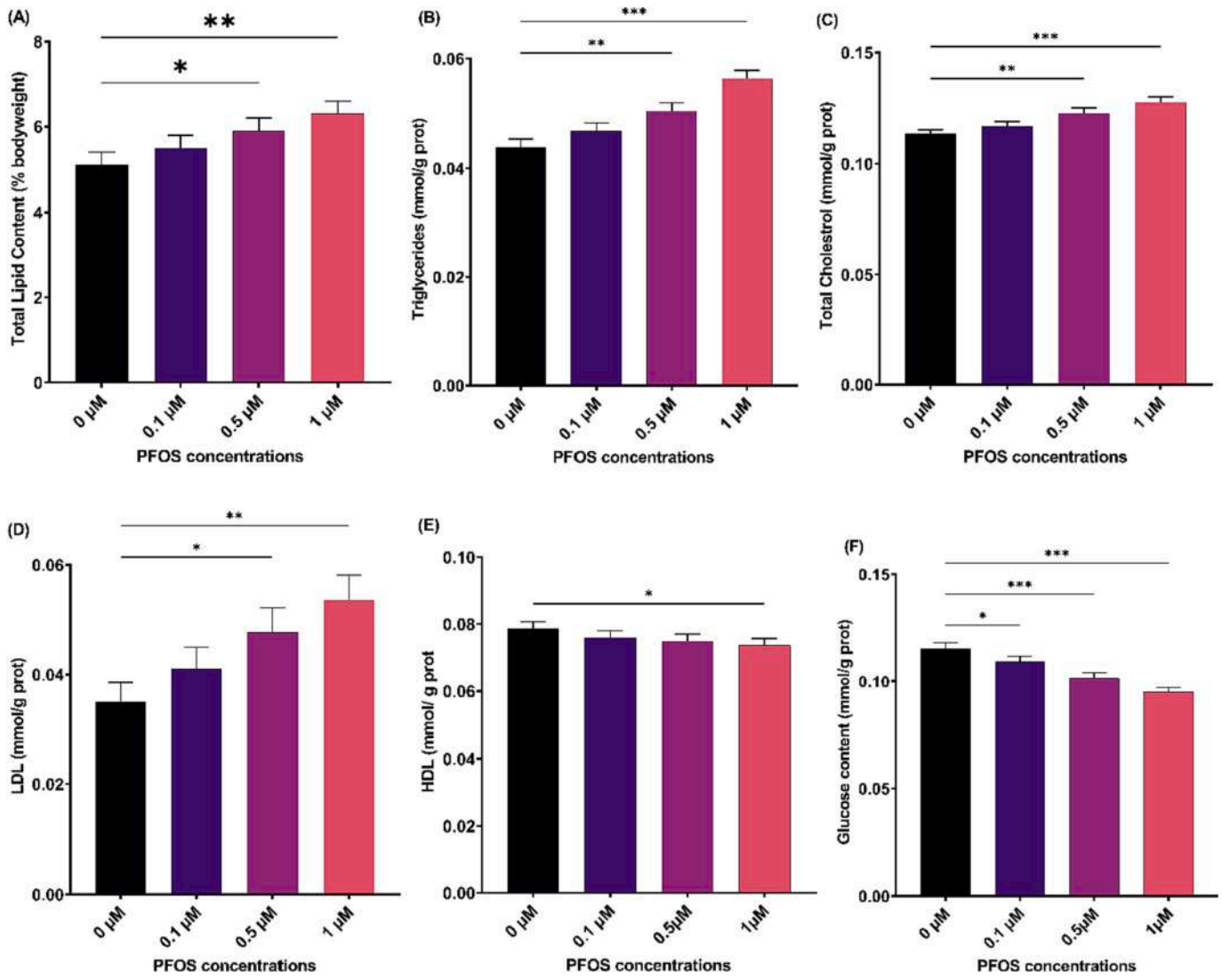

Fig. 4. Total lipid content (A), triglycerides (B), total cholesterol (C), LDL (D), HDL (E), and glucose content (F) of zebrafish embryos exposed to PFOS concentrations. Values represented as mean ± SD. Significance levels: $P < 0.05$, $P < 0.01$, and $P < 0.001$ denoted by *, **, and ***, respectively.

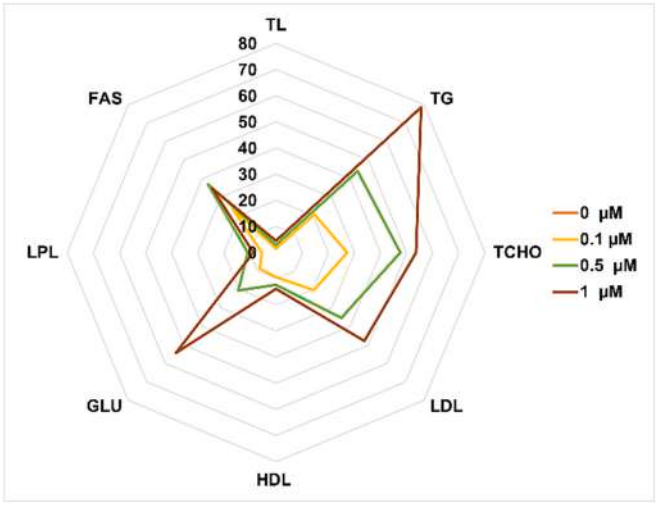

Fig. 5. IBRv2 star plot of several biochemical markers of lipid metabolism after PFOS exposure.

4. Discussion

The present study demonstrated that PFOS exposure during embryonic period caused various developmental toxicity by inducing aberrant lipid metabolism and disruption of neurotransmission. Developing organisms are always susceptible to any kind of environmental toxins and hence may pose a potential threat to aquatic ecosystems. In our study, developmental toxicity induced by PFOS in zebrafish was indicated by hatching rate, mortality rate, morphology score, and malformation rate in zebrafish larvae in a dose-dependent manner. These results have shown that PFOS can cause remarkable developmental abnormalities in zebrafish larvae including delayed hatching (48–96 hpf), increased mortality and malformation rate which was consisted with a previous study (Chen et al., 2020). Briefly, hatching is considered as the critical window period for zebrafish embryogenesis. The consequences of delayed hatching might be the retarded or inability to come out of the chorions and sometimes eventually led to death of embryos also (Gupta et al., 2023; Mahapatra et al., 2023). Therefore, the differences in hatching (%) and mortality (%) after PFOS exposure shows slower development of zebrafish embryos (Zhang et al., 2015). The yolk sac is essential during the early development stage since it is the primary source of sustenance for embryos, and its physical size decreases as the embryo develops. Lesser or fewer deformities were seen in control

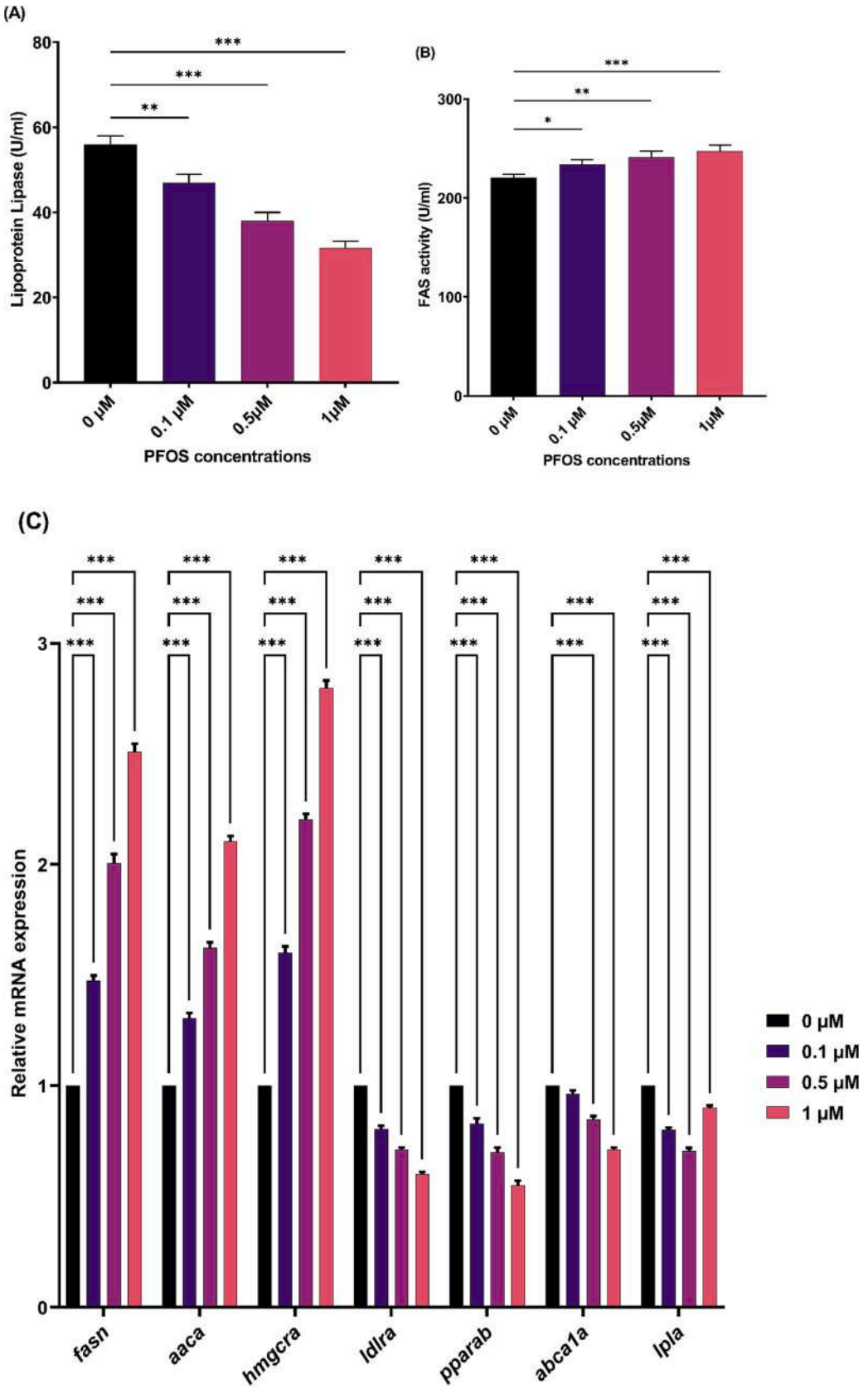

Fig. 6. (A) LPL and (B) FAS activity in 96 hpf larvae homogenate after PFOS exposure. (C) The relative fold change in expression of genes involved in lipid metabolism as measured by qRT-PCR. Values represented as mean ± SD. Significance levels: $P < 0.05$, $P < 0.01$, and $P < 0.001$ denoted by *, **, and ***, respectively.

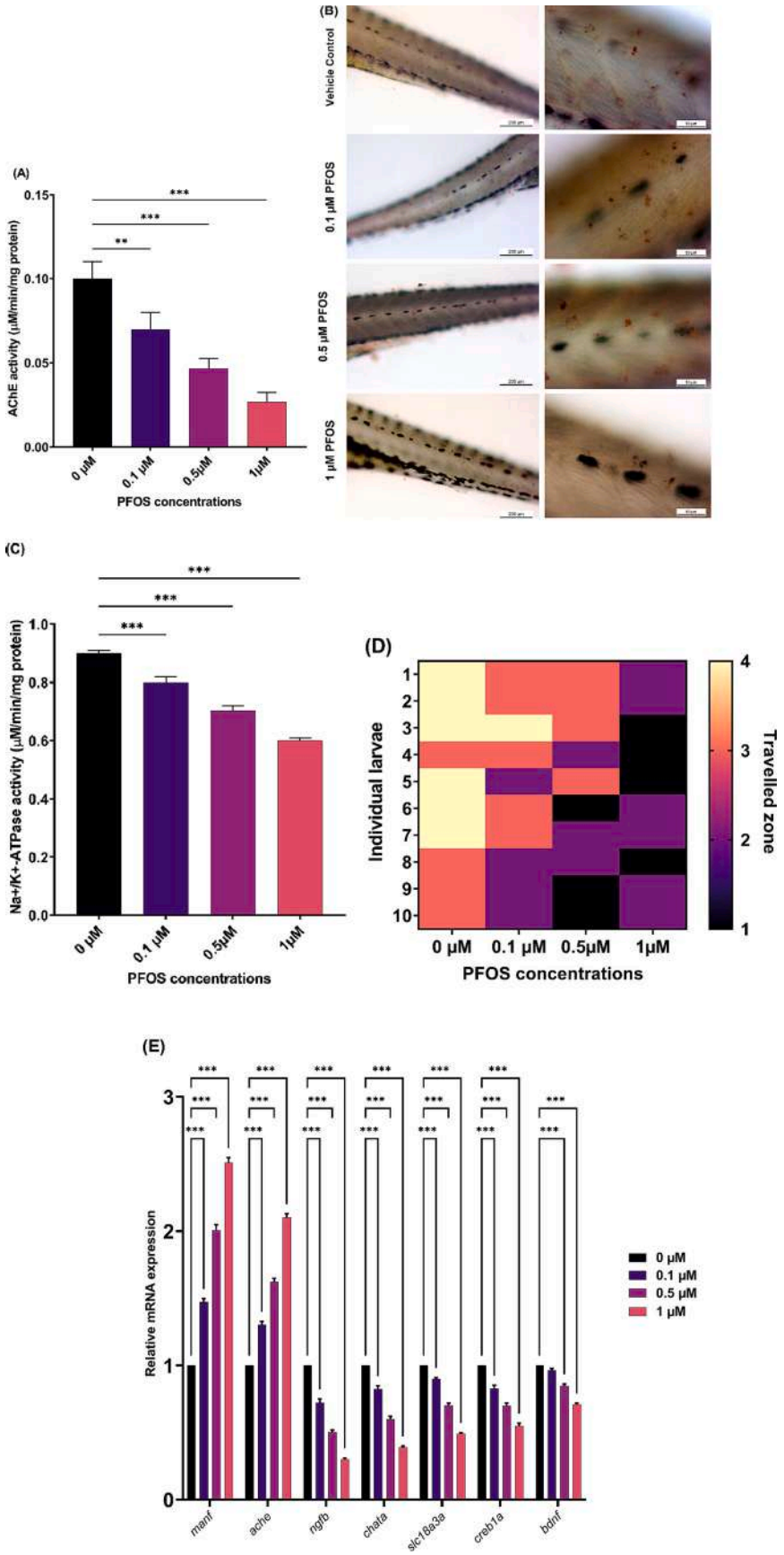

Fig. 7. (A) AChE activity, (B) representative images of AChE localization in 96 hpf zebrafish embryos following exposure, (C) Na^{+}/K^{+}-ATPase activity and (D) heat map showing traveled zone by individual larvae from different experimental groups. (E) The relative fold change in expression of genes involved in *manf-ache* pathway as measured by qRT-PCR. Values represented as mean ± SD. Significance levels: $P < 0.05$, $P < 0.01$, and $P < 0.001$ denoted by *, **, and ***, respectively.

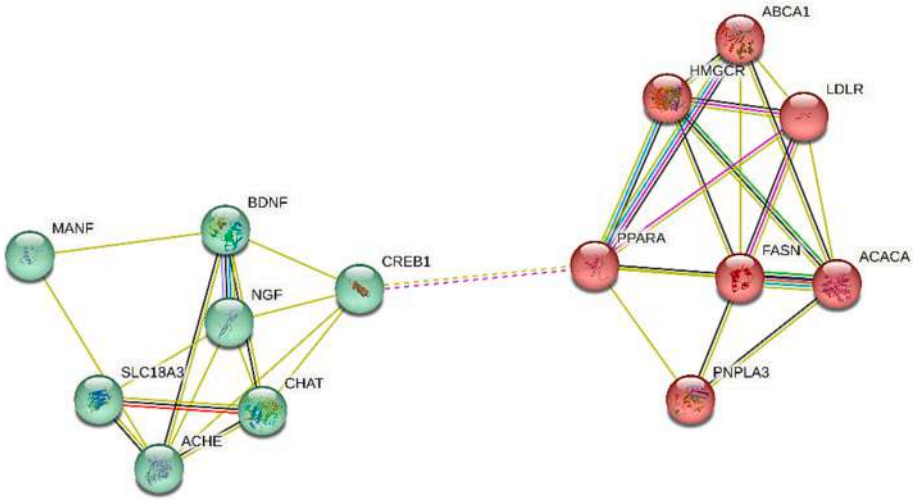

Fig. 8. STRING Protein-Protein Interaction analysis showing interaction between proteins (of respective genes) of our interest.

group, but the treated group showed increased YSE, PE, bent body axis curvature and tail malformations. These results showed that PFOS can considerably impede zebrafish embryo development.

ORO stains neutral lipids and TGs (Mehlem et al., 2013), therefore the quantitative measurement of ORO staining can be a direct assessment of neutral lipid and TGs content (Yogananthajah et al., 2017). As in our study, ORO staining after PFOS exposure have shown increased content of neutral lipid and TGs as further demonstrated by quantification analysis that suggests disruption in neutral lipid mobilization from the zebrafish embryonic yolk sac. Consistent with our findings, same pattern was observed in zebrafish embryos after PFOA and its novel analogs exposure (Sun et al., 2023).

In general, as the fish embryos hatch out, the depletion of lipid from yolk sac starts for nutrition (Wiegand, 1996). Quantification of total lipid demonstrated that lipid content was accumulated in zebrafish larvae after PFOS exposure. Earlier study has shown that difenoconazole exposure in marine medaka resulted in increased content of total lipids (Dong et al., 2016) and subsequently increased TG level in embryonic zebrafish after 96 h (Hu et al., 2016). In fact, TG and TCHO are considered as the important biomarkers for indicating any lipid metabolism disorders. TGs constitute a prominent class of neutral lipids that supply most of the energy ingested by embryo throughout the growth and development. Meanwhile, cholesterol is the most common tetracyclic hydrocarbon compounds, exists as a crucial component of cell membranes (Simons and Ikonen, 1997) and provides protection of membrane lipids (Zhang et al., 2018). It is also essential for transport and signal transduction between cells (Mu et al., 2015; Simons and Toomre, 2000) or it can exist in a neutral lipid storage form esterified to a fatty acid (Kojima et al., 2009). The present findings showed an appreciable increase in TCHO, TGs and total lipid content in the highest dose group (Qian et al., 2018; Yan et al., 2022).

Lipid metabolism plays a major role during early-life stages of zebrafish embryo development (Teng et al., 2019). FAS is a key enzyme present in the cytoplasm that catalyzes lipogenesis from glucose and therefore increases in de novo fatty acid synthesis (Qian et al., 2018). LPL is a triacylglycerol hydrolase that hydrolyses TG in circulating lipoproteins (Goldberg et al., 1986). The rate-limiting step for the adsorption of TG produced from FA is defined as the degree of LPL expression in a specific tissue. In our study, there was a decrease in level of LPL enzyme which is consistent with the observed increase in total lipid and TG content. This result indicates that due to decrease in LPL activity and increase in FAS, there will be decrease in breakdown of circulating TG, and hence resulting in increased accumulation of total lipid and TG in zebrafish embryos (Zhang et al., 2019). In our study, the observed increase in TCHO and LDL cholesterol can be demonstrated by the PFOS effect on cholesterol synthesis and uptake. As earlier shown that FAS activity increased after exposure which is in accordance with the increase in TCHO production levels. Similarly, PFOS might be inhibiting the uptake of LDL cholesterol and hence there is increased level of LDL cholesterol in exposed zebrafish embryos. However, HDL plays protective role against cardiovascular diseases and a decrease in its level could be associated with increased risk of diseases as observed in our study.

Lipid homeostasis is governed by significant number of genes including lipid intake, mobilization, storage, synthesis, metabolism, and breakdown. Therefore, there should be a proper mechanism to maintain and regulate the optimal lipid homeostasis either at the transcriptional or protein level in response to feedback signals (Tocher, 2003). For instance, Peroxisome proliferator-activated receptor (PPARs) family are clusters of nuclear receptors that play a key role in lipid metabolism, such as fatty acid oxidation, biosynthesis, and uptake. There are three isoforms of PPAR: PPARα, PPARβ/δ, and PPARγ, each of which has distinct functions in lipid metabolism acting as either sensor or signal transducers (Mylroie et al., 2021). In the current study, we have showed that PFOS exposure resulted in decrease gene expression of PPARα indicating decreased fatty acid β-oxidation which regulates biological processes during development and growth of the organisms (la Poulsen et al., 2012). Subsequently, lipases are involved in breakdown of lipids including TGs and phospholipids (Heindel et al., 2017). The present study demonstrated that *lpla* was downregulated and therefore the breakdown of TGs or TGs uptake from blood was decreased and hence there is accumulation of TGs as demonstrated in our findings. Furthermore, Fatty acid synthase (FASN) and Acetyl-CoA carboxylase alpha (ACACA) plays central roles in fatty acid metabolism. In the current study, there is increased expression level of *fasn* and *acaca* which suggest an increase in de novo fatty acid synthesis and regulation of fatty acid synthesis respectively (Yu et al., 2020). This might contribute to the rise in TLs, TCHO, and TGs which is remarkably found in our study. The genes involved in cholesterol metabolism include 3-hydroxy-3-methylglutaryl-CoA reductase (HMCGR), which is the rate-limiting enzyme in cholesterol synthesis, and low-density lipoprotein receptor (LDLR), responsible for uptake of LDL cholesterol from the bloodstream (O'Hare et al., 2014). The altered expression of *hmgcra* and *ldlra* suggests that there is imbalance in the clearance of lipoproteins. Moreover, ATP-binding cassette transporter A1 (*abca1a*) expression gets significantly downregulated due to decreased level of HDL cholesterol (Xu et al., 2017).

Overall, the observed abnormalities in lipid metabolism indicate that PFOS is interfering with lipid metabolism pathways, including lipolysis, lipogenesis, cholesterol production, and cholesterol absorption. Further

research would be needed to discover the specific molecular pathways involved and the possible ramifications of these alterations in lipid metabolism for the health of aquatic organisms exposed to PFOS.

Acetylcholine (ACh) is the major neurotransmitter of the cholinergic system and plays a crucial role in central and neuromuscular synapses (Behra et al., 2002; Suman et al., 2023). In the central nervous system, these cholinergic neurons are widely distributed and therefore responsible for modulating neurological functions. Experimental evidence has shown that injuries introduced in forebrain cholinergic neurons led to attention deficit (Ferreira-Vieira et al., 2016). During cholinergic signaling in the nervous system, ACh releases from the pre-synaptic nerve terminals and binds to its receptor which are present in post-synaptic membrane. After release, ACh are rapidly degraded by AChE and cleaves ACh into choline and acetate. Therefore, the AChE has been underscored as an important biomarker for neurotoxicity exposure in aquatic organisms (Wang et al., 2019b). As in our study, PFOS exposure has shown decreased activity of AChE enzyme which resulted in accumulation of acetylcholine neurotransmitter in synaptic cleft and therefore ultimately resulting in enhanced cholinergic transmission. This can result in overstimulation of cholinergic neurons and, as a result, a decrease in responsiveness, leads to hypoactive muscle contraction and behavioral actions (Chen et al., 2012). Consistent with these, in our study also, PFOS exposure resulted in deceased AChE activity and eventually impaired TEE. The delayed response in TEE is one of the important biological endpoints for neurotoxicity evaluation (Wang et al., 2019a). The present work observed delayed TEE in exposed groups in a dose-dependent manner indicating PFOS induces neurotoxicity. This finding agreed with the previous studies that reported inhibition of AChE activity might cause altered behavior, eventually leading to neurodevelopmental toxicity in zebrafish larvae (Chen et al., 2012). Additionally, Na^+/K^+-ATPase is an ion pump that is critical for maintaining proper ion concentrations and electrical gradients across cell membranes (Wang et al., 2020). The decrease in enzymatic activity of Na^+/K^+-ATPase can lead to an imbalance of ion gradients across neuronal membranes, resulting into altered neuronal excitability and potential neurotoxic effects as demonstrated in our experiment (Gupta et al., 2023; Mahapatra et al., 2022). Taken together, these findings suggest that PFOS might be interfering with cholinergic signaling and ion transport processes in neurons.

In terms of molecular mechanism, alteration of several genes involved in *manf-ache* pathway might be responsible for development neurotoxicity after PFOS exposure. The transcript level of *manf* was increased in embryonic zebrafish after PFOS exposure. Among all the genes, increased *ache* activity and downregulated choline acetyltransferase (*chata*) genes were found in PFOS-exposed zebrafish larvae. CHAT is responsible for synthesizing acetylcholine in neurons (Granger et al., 2020) and therefore PFOS induced accumulation of acetylcholine occurs after downregulation of its expression. The gene nerve-growth factor (*ngfb*) and brain-derived neurotrophic factor (*bdnf*) are involved in promoting survival and growth of cholinergic neurons (Allen et al., 2013). PFOS dysregulates the gene expression of *ngfb* and *bdnf* and hence potentially contributing to neurotoxic effects (Wu et al., 2017). Vesicular acetylcholine transporter (*slc18a3a*) transports acetylcholine into synaptic vesicles for secretion. cAMP response element-binding protein (*creb1a*) is a transcription factor that plays a role in regulating gene expression in response to synaptic activity. The decreased level of *slc18a3a* and *creb1a* shows dysregulation in other cholinergic and ion transport genes. Concludingly, these results indicate that PFOS induced adverse effect on neurodevelopment by affecting the key genes involved in early life-stage of zebrafish. STRING protein-protein interaction is showing that how lipid metabolism and cholinergic neurotransmission is correlated with each other through *pparα-creb1* pathway.

In summary, this research provides an extensive evaluation of the impact of PFOS exposure on the early life stages of zebrafish, encompassing the effects on developmental abnormalities, lipid metabolism, and neurotoxicity endpoints. Our study reveals that PFOS exposure is associated with developmental anomalies, such as delayed hatching and increased mortality, as well as changes in lipid metabolism, including altered enzyme activity and lipid droplet formation. Moreover, our findings demonstrate that PFOS exposure induces neurotoxicity, as shown by changes in the activity and staining of the AChE enzyme, TEE, Na^+/K^+-ATPase enzyme activity, and the expression of crucial neuronal markers. Overall, this research emphasizes the necessity of assessing the impact of environmental pollutants, such as PFOS, on developing organisms. Given that zebrafish embryos and larvae are widely used as model organisms in toxicology and developmental biology research, our results have significant implications for comprehending the potential health risks of PFOS exposure in human populations. Ultimately, a better understanding of the mechanisms underlying the observed effects of PFOS on zebrafish embryos and larvae could aid in the development of effective measures to mitigate the health hazards linked to exposure to PFOS and other environmental pollutants.

5. Conclusion

This study provides important insights into the potential adverse health effects of PFOS exposure on developing zebrafish embryos. The results demonstrate that PFOS exposure alters lipid and glucose parameters, as well as key molecular mechanisms underlying neurological development and function. The dyslipidemic effects of PFOS exposure observed in this study, including the increase in TLs, TGs, TCHO, and LDL cholesterol, and the decrease in HDL cholesterol, suggest an increased risk of cardiovascular disease. Additionally, the study's finding of a significant decrease in glucose levels suggests that PFOS exposure may impair glucose metabolism. The observed alterations in lipid metabolism and gene expression suggest that PFOS exposure alters lipid uptake and metabolism, stimulates de novo fatty acid synthesis, and inhibits cholesterol uptake and transport. Additionally, the altered key molecular mechanisms underlying neurological development and function, including cholinergic neurotransmission, neuronal plasticity, and ion homeostasis, underscore the potential neurotoxicity of PFOS exposure. Moreover, the correlation between lipid levels and acetylcholinesterase activity has been observed though STRING network analysis. These findings highlight the urgent need for further research to fully elucidate the underlying molecular mechanisms and potential long-term effects of PFOS exposure, and to inform the development of effective preventive and therapeutic strategies to minimize the public health threat posed by PFOS exposure.

Supplementary data to this article can be found online at https://doi.org/10.1016/j.ntt.2023.107304.

Declaration of Competing Interest

The authors declare the following financial interests/personal relationships which may be considered as potential competing interests.

Rahul Kumar Singh reports financial support was provided by Science and Engineering Research Board. Rahul Kumar Singh reports financial support was provided by State Council of Science and Technology Uttar Pradesh. Rahul Kumar Singh reports a relationship with Banaras Hindu University that includes: employment.

Data availability

Data will be made available on request.

Acknowledgments

This work was supported by Science and Engineering Research Board, New Delhi (ECR/2017/000685); Council of Science and Technology, Uttar Pradesh (CST/D-2300), Institution of Eminence (IoE), BHU (OH 31-IoE) for grants to RKS, UGC-CSIR for Senior Research Fellowships to AM, PG, AS, and ICMR for Senior Research Fellowship to

SSR. We are highly indebted to CAS, ISLS, SATHI, CDC facilities of BHU and Dr. Raghav Mishra and Dr. Ajit Singh, Zoology, BHU for providing instrumental facilities.

References

Alecu, I., Bennett, S.A.L., 2019. Dysregulated Lipid Metabolism and Its Role in α-Synucleinopathy in Parkinson's Disease. Front. Neurosci. 13, 328. https://doi.org/10.3389/fnins.2019.00328.

Al-Jamal, O., Al-Jighefee, H., Younes, N., Abdin, R., Al-Asmakh, M.A., Radwan, A.B., Sliem, M.H., Majdalawieh, A.F., Pintus, G., Yassine, H.M., Abdullah, A.M., Da'as, S. I., Nasrallah, G.K., 2020. Organ-specific toxicity evaluation of stearamidopropyl dimethylamine (SAPDMA) surfactant using zebrafish embryos. Sci. Total Environ. 741, 140450 https://doi.org/10.1016/j.scitotenv.2020.140450.

Allen, S.J., Watson, J.J., Shoemark, D.K., Barua, N.U., Patel, N.K., 2013. GDNF, NGF and BDNF as therapeutic options for neurodegeneration. Pharmacol. Ther. 138, 155–175. https://doi.org/10.1016/j.pharmthera.2013.01.004.

Basnet, R.M., Guarienti, M., Memo, M., 2017. Zebrafish embryo as an in vivo model for behavioral and pharmacological characterization of Methylxanthine drugs. Int. J. Mol. Sci. https://doi.org/10.3390/ijms18030596.

Behra, M., Cousin, X., Bertrand, C., Vonesch, J.-L., Biellmann, D., Chatonnet, A., Strähle, U., 2002. Acetylcholinesterase is required for neuronal and muscular development in the zebrafish embryo. Nat. Neurosci. 5, 111–118. https://doi.org/10.1038/nn788.

Beliaeff, B., Burgeot, T., 2002. Integrated biomarker response: a useful tool for ecological risk assessment. Environ. Toxicol. Chem. 21, 1316–1322.

Bradford, M.M., 1976. A rapid and sensitive method for the quantitation of microgram quantities of protein utilizing the principle of protein-dye binding. Anal. Biochem. 72, 248–254.

Caliani, I., Campani, T., Conti, B., Cosci, F., Bedini, S., D'Agostino, A., Ammendola, A., Di Noi, A., Gori, A., Casini, S., 2021. Multi-biomarker approach and IBR index to evaluate the effects of different contaminants on the ecotoxicological status of Apis mellifera. Ecotoxicol. Environ. Saf. 208, 111486 https://doi.org/10.1016/j.ecoenv.2020.111486.

Chen, L., Yu, K., Huang, C., Yu, L., Zhu, B., Lam, P.K.S., Lam, J.C.W., Zhou, B., 2012. Prenatal transfer of polybrominated diphenyl ethers (PBDEs) results in developmental neurotoxicity in zebrafish larvae. Environ. Sci. Technol. 46, 9727–9734. https://doi.org/10.1021/es302119g.

Chen, N., Li, J., Li, D., Yang, Y., He, D., 2014. Chronic exposure to Perfluorooctane sulfonate induces behavior defects and neurotoxicity through oxidative damages, in vivo and in vitro. PLoS One 9, e113453.

Chen, G., Wang, L., Li, W., Zhang, Q., Hu, T., 2020. Nodularin induced oxidative stress contributes to developmental toxicity in zebrafish embryos. Ecotoxicol. Environ. Saf. 194, 110444.

Chia, K., Klingseisen, A., Sieger, D., Priller, J., 2022. Zebrafish as a model organism for neurodegenerative disease. Frontiers in molecular neuroscience 15, 940484. https://doi.org/10.3389/fnmol.2022.940484.

Clark, R.B., Dick, J.E., 2020. Electrochemical sensing of Perfluorooctanesulfonate (PFOS) using ambient oxygen in river water. ACS Sens. 5, 3591–3598. https://doi.org/10.1021/acssensors.0c01894.

Cousins, I.T., Johansson, J.H., Salter, M.E., Sha, B., Scheringer, M., 2022. Outside the safe operating space of a new planetary boundary for per- and Polyfluoroalkyl substances (PFAS). Environ. Sci. Technol. 56, 11172–11179. https://doi.org/10.1021/acs.est.2c02765.

Dai, L., Zou, L., Meng, L., Qiang, G., Yan, M., Zhang, Z., 2021. Cholesterol Metabolism in Neurodegenerative Diseases: Molecular Mechanisms and Therapeutic Targets. Mol. Neurobiol. 58 (5), 2183–2201. https://doi.org/10.1007/s12035-020-02232-6.

Di Paola, D., Capparucci, F., Abbate, J.M., Cordaro, M., Crupi, R., Siracusa, R., D'Amico, R., Fusco, R., Genovese, T., Impellizzeri, D., Cuzzocrea, S., Spanò, N., Gugliandolo, E., Peritore, A.F., 2022. Environmental risk assessment of Oxaliplatin exposure on early life stages of zebrafish (Danio rerio). Toxics. https://doi.org/10.3390/toxics10020081.

Dong, X., Li, Y., Zhang, L., Zuo, Z., Wang, C., Chen, M., 2016. Influence of difenoconazole on lipid metabolism in marine medaka (Oryzias melastigma). Ecotoxicology 25, 982–990. https://doi.org/10.1007/s10646-016-1655-5.

Ellman, G.L., Courtney, K.D., Andres Jr., V., Featherstone, R.M., 1961. A new and rapid colorimetric determination of acetylcholinesterase activity. Biochem. Pharmacol. 7, 88–95.

Ferreira-Vieira, T.H., Guimaraes, I.M., Silva, F.R., Ribeiro, F.M., 2016. Alzheimer's disease: targeting the cholinergic system. Curr. Neuropharmacol. 14, 101–115. https://doi.org/10.2174/1570159x13666150716165726.

Folch, J., 1941. The isolation of phosphatidyl serine from brain cephalin, and identification of the serine component. J. Biol. Chem. 139, 973–974.

Goldberg, I.J., Kandel, J.J., Blum, C.B., Ginsberg, H.N., 1986. Association of plasma lipoproteins with postheparin lipase activities. J. Clin. Invest. 78, 1523–1528. https://doi.org/10.1172/JCI112744.

Granger, A.J., Wang, W., Robertson, K., El-Rifai, M., Zanello, A.F., Bistrong, K., Saunders, A., Chow, B.W., Nuñez, V., Turrero García, M., Harwell, C.C., Gu, C., Sabatini, B.L., 2020. Cortical ChAT+ neurons co-transmit acetylcholine and GABA in a target- and brain-region-specific manner. Elife 9, e57749. https://doi.org/10.7554/eLife.57749.

Guo, M., Wu, F., Geng, Q., Wu, H., Song, Z., Zheng, G., Peng, J., Zhao, X., Tan, Z., 2023. Perfluoroalkyl substances (PFASs) in aquatic products from the yellow-Bohai Sea coasts, China: concentrations and profiles across species and regions. Environ. Pollut. 121514 https://doi.org/10.1016/j.envpol.2023.121514.

Gupta, P., Mahapatra, A., Suman, A., Ray, S.S., Malafaia, G., Singh, R.K., 2023. Polystyrene microplastics disrupt female reproductive health and fertility via sirt1 modulation in zebrafish (Danio rerio). J. Hazard. Mater. 460, 132359. https://doi.org/10.1016/j.jhazmat.2023.132359.

Gupta, P., Mahapatra, A., Suman, A., Singh, R.K., 2023. In silico and in vivo assessment of developmental toxicity, oxidative stress response & Na+/K+-ATPase activity in zebrafish embryos exposed to cypermethrin. Ecotoxicol. Environ. Saf. 251, 114547 https://doi.org/10.1016/j.ecoenv.2023.114547.

Hallberg, I., Kjellgren, J., Persson, S., Örn, S., Sjunnesson, Y., 2019. Perfluorononanoic acid (PFNA) alters lipid accumulation in bovine blastocysts after oocyte exposure during in vitro maturation. Reprod. Toxicol. 84, 1–8. https://doi.org/10.1016/j.reprotox.2018.11.005.

Heindel, J.J., Blumberg, B., Cave, M., Machtinger, R., Mantovani, A., Mendez, M.A., Nadal, A., Palanza, P., Panzica, G., Sargis, R., Vandenberg, L.N., vom Saal, F., 2017. Metabolism disrupting chemicals and metabolic disorders. Reprod. Toxicol. 68, 3–33. https://doi.org/10.1016/j.reprotox.2016.10.001.

Hill, J.B., Kessler, G., 1961. An automated determination of glucose utilizing a glucose oxidase-peroxidase system. J. Lab. Clin. Med. 57, 970–980. https://doi.org/10.5555/uri:pii:0022214361900993.

Hu, L., Su, L., Xue, Y., Mu, J., Zhu, J., Xu, J., Shi, H., 2016. Uptake, accumulation and elimination of polystyrene microspheres in tadpoles of Xenopus tropicalis. Chemosphere 164, 611–617. https://doi.org/10.1016/j.chemosphere.2016.09.002.

Jantzen, C.E., Annunziato, K.M., Cooper, K.R., 2016. Behavioral, morphometric, and gene expression effects in adult zebrafish (Danio rerio) embryonically exposed to PFOA, PFOS, and PFNA. Aquat. Toxicol. 180, 123–130. https://doi.org/10.1016/j.aquatox.2016.09.011.

Karnovsky, M.J., Roots, L., 1964. A" direct-coloring" thiocholine method for cholinesterases. J. Histochem. Cytochem. 12, 219–221.

Kojima, M., Ashino, T., Yoshida, T., Iwakura, Y., Sekimoto, M., Degawa, M., 2009. IL-1 regulates the Cyp7a1 gene and serum total cholesterol level at steady state in mice. Biochem. Biophys. Res. Commun. 379, 239–242. https://doi.org/10.1016/j.bbrc.2008.12.032.

la Poulsen, L.C., Siersbæk, M., Mandrup, S., 2012. PPARs: fatty acid sensors controlling metabolism. Semin. Cell Dev. Biol. 23, 631–639. https://doi.org/10.1016/j.semcdb.2012.01.003.

Liang, L., Pan, Y., Bin, L., Liu, Y., Huang, W., Li, R., Lai, K.P., 2022. Immunotoxicity mechanisms of perfluorinated compounds PFOA and PFOS. Chemosphere 291, 132892. https://doi.org/10.1016/j.chemosphere.2021.132892.

Livak, K.J., Schmittgen, T.D., 2001. Analysis of relative gene expression data using real-time quantitative PCR and the 2(-Delta Delta C(T)) Method. *Methods (San Diego.* Calif.) 25 (4), 402–408. https://doi.org/10.1006/meth.2001.1262.

Mahapatra, A., Gupta, P., Suman, A., Ray, S.S., Malafaia, G., Singh, R.K., 2023. Unraveling the mechanisms of perfluorooctanesulfonic acid-induced dopaminergic neurotoxicity and microglial activation in developing zebrafish. Sci. Total Environ. 887, 164030. https://doi.org/10.1016/j.scitotenv.2023.164030.

Mahapatra, A., Mistri, A., Gupta, P., Kar, S., Mittal, S., Singh, R.K., 2022. Toxicopathological impact of sub-lethal concentrations of lead nitrate on the gill of the catfish Heteropneustes fossilis. Acta Histochem. 124, 151848.

Mehlem, A., Hagberg, C.E., Muhl, L., Eriksson, U., Falkevall, A., 2013. Imaging of neutral lipids by oil red O for analyzing the metabolic status in health and disease. Nat. Protoc. 8, 1149–1154. https://doi.org/10.1038/nprot.2013.055.

Menger, F., Pohl, J., Ahrens, L., Carlsson, G., Örn, S., 2020. Behavioural effects and bioconcentration of per- and polyfluoroalkyl substances (PFASs) in zebrafish (Danio rerio) embryos. Chemosphere 245, 125573. https://doi.org/10.1016/j.chemosphere.2019.125573.

Mshaty, A., Haijima, A., Takatsuru, Y., Ninomiya, A., Yajima, H., Kokubo, M., Khairinisa, M.A., Miyazaki, W., Amano, I., Koibuchi, N., 2020. Neurotoxic effects of lactational exposure to perfluorooctane sulfonate on learning and memory in adult male mouse. Food Chem. Toxicol. 145, 111710 https://doi.org/10.1016/j.fct.2020.111710.

Mu, X., Wang, K., Chai, T., Zhu, L., Yang, Y., Zhang, J., Pang, S., Wang, C., Li, X., 2015. Sex specific response in cholesterol level in zebrafish (Danio rerio) after long-term exposure of difenoconazole. Environ. Pollut. 197, 278–286. https://doi.org/10.1016/j.envpol.2014.11.019.

Mylroie, J.E., Wilbanks, M.S., Kimble, A.N., To, K.T, Cox, C.S., McLeod, S.J., Gust, K.A., Moore, D.W., Perkins, E.J., Garcia-Reyero, N., 2021. Perfluorooctanesulfonic Acid–Induced Toxicity on Zebrafish Embryos in the Presence or Absence of the Chorion. Environ. Toxicol. Chem. 40, 780–791. https://doi.org/10.1002/etc.4899.

O'Hare, E.A., Wang, X., Montasser, M.E., Chang, Y.-P.C., Mitchell, B.D., Zaghloul, N.A., 2014. Disruption of ldlr causes increased LDL-c and vascular lipid accumulation in a zebrafish model of hypercholesterolemia [S]. J. Lipid Res. 55, 2242–2253. https://doi.org/10.1194/jlr.M046540.

Panzica-Kelly, J.M., Zhang, C.X., Danberry, T.L., Flood, A., DeLan, J.W., Brannen, K.C., Augustine-Rauch, K.A., 2010. Morphological score assignment guidelines for the dechorionated zebrafish teratogenicity assay. Birth Defects Res. B. Dev. Reprod. Toxicol. 89, 382–395. https://doi.org/10.1002/bdrb.20260.

Qian, L., Cui, F., Yang, Y., Liu, Y., Qi, S., Wang, C., 2018. Mechanisms of developmental toxicity in zebrafish embryos (Danio rerio) induced by boscalid. Sci. Total Environ. 634, 478–487.

Rea, V., Van Raay, T.J., 2020. Using Zebrafish to Model Autism Spectrum Disorder: A Comparison of ASD Risk Genes Between Zebrafish and Their Mammalian Counterparts. Front. Mol. Neurosci. 13, 575575. https://doi.org/10.3389/fnmol.2020.575575.

Shi, X., Du, Y., Lam, P.K., Wu, R.S., Zhou, B., 2008. Developmental toxicity and alteration of gene expression in zebrafish embryos exposed to PFOS. Toxicol. Appl. Pharmacol. 230 (1), 23–32. https://doi.org/10.1016/j.taap.2008.01.043.

Simons, K., Ikonen, E., 1997. Functional rafts in cell membranes. Nature 387, 569–572. https://doi.org/10.1038/42408.

Simons, K., Toomre, D., 2000. Lipid rafts and signal transduction. Nat. Rev. Mol. Cell Biol. 1, 31–39. https://doi.org/10.1038/35036052.

Suman, A., Mahapatra, A., Gupta, P., Ray, S.S., Singh, R.K., 2023. Polystyrene microplastics modulated bdnf expression triggering neurotoxicity via apoptotic pathway in zebrafish embryos. *Comparative biochemistry and physiology*. Toxicol. Pharmacol.: CBP 271, 109699. https://doi.org/10.1016/j.cbpc.2023.109699.

Sun, P., Nie, X., Chen, X., Yin, L., Luo, J., Sun, L., Wan, C., Jiang, S., 2018. Nrf2 signaling elicits a neuroprotective role against PFOS-mediated oxidative damage and apoptosis. Neurochem. Res. 43, 2446–2459. https://doi.org/10.1007/s11064-018-2672-y.

Sun, W., Zhang, X., Qiao, Y., Griffin, N., Zhang, H., Wang, L., Liu, H., 2023. Exposure to PFOA and its novel analogs disrupts lipid metabolism in zebrafish. Ecotoxicol. Environ. Saf. 259, 115020 https://doi.org/10.1016/j.ecoenv.2023.115020.

Tan, F., Jin, Y., Liu, W., Quan, X., Chen, J., Liang, Z., 2012. Global liver proteome analysis using iTRAQ labeling quantitative proteomic technology to reveal biomarkers in mice exposed to perfluorooctane sulfonate (PFOS). Environ. Sci. Technol. 46, 12170–12177. https://doi.org/10.1021/es3027715.

Teng, M., Zhao, F., Zhou, Y., Yan, S., Tian, S., Yan, J., Meng, Z., Bi, S., Wang, C., 2019. Effect of Propiconazole on the lipid metabolism of zebrafish embryos (Danio rerio). J. Agric. Food Chem. 67, 4623–4631. https://doi.org/10.1021/acs.jafc.9b00449.

Tocher, D.R., 2003. Metabolism and functions of lipids and fatty acids in teleost fish. Rev. Fish. Sci. 11, 107–184. https://doi.org/10.1080/713610925.

Wan, H.T., Zhao, Y.G., Wei, X., Hui, K.Y., Giesy, J.P., Wong, C.K., 2012. PFOS-induced hepatic steatosis, the mechanistic actions on β-oxidation and lipid transport. Biochim. Biophys. Acta 1820 (7), 1092–1101. https://doi.org/10.1016/j.bbagen.2012.03.010.

Wang, S., Duan, M., Guan, K., Zhou, X., Zheng, M., Shi, X., Ye, M., Guan, W., Kuver, A., Huang, M., Liu, Y., Dai, K., Li, X., 2019a. Developmental neurotoxicity of reserpine exposure in zebrafish larvae (Danio rerio). Comp. Biochem. Physiol. C. Toxicol. Pharmacol. 223, 115–123. https://doi.org/10.1016/j.cbpc.2019.05.008.

Wang, H., Zhou, L., Liao, X., Meng, Z., Xiao, J., Li, F., Zhang, S., Cao, Z., Lu, H., 2019b. Toxic effects of oxine-copper on development and behavior in the embryo-larval stages of zebrafish. Aquat. Toxicol. 210, 242–250. https://doi.org/10.1016/j.aquatox.2019.02.020.

Wang, H., Meng, Z., Liu, F., Zhou, L., Su, M., Meng, Y., Zhang, S., Liao, X., Cao, Z., Lu, H., 2020. Characterization of boscalid-induced oxidative stress and neurodevelopmental toxicity in zebrafish embryos. Chemosphere 238, 124753. https://doi.org/10.1016/j.chemosphere.2019.124753.

Wiegand, M.D., 1996. Composition, accumulation and utilization of yolk lipids in teleost fish. Rev. Fish Biol. Fish. 6, 259–286. https://doi.org/10.1007/BF00122583.

Wu, Q., Yan, W., Cheng, H., Liu, C., Hung, T.-C., Guo, X., Li, G., 2017. Parental transfer of microcystin-LR induced transgenerational effects of developmental neurotoxicity in zebrafish offspring. Environ. Pollut. 231, 471–478. https://doi.org/10.1016/j.envpol.2017.08.038.

Xu, E.G., Mager, E.M., Grosell, M., Hazard, E.S., Hardiman, G., Schlenk, D., 2017. Novel transcriptome assembly and comparative toxicity pathway analysis in mahi-mahi (Coryphaena hippurus) embryos and larvae exposed to Deepwater horizon oil. Sci. Rep. 7, 44546. https://doi.org/10.1038/srep44546.

Xu, M., Legradi, J., Leonards, P., 2022. Using comprehensive lipid profiling to study effects of PFHxS during different stages of early zebrafish development. Sci. Total Environ. 808, 151739 https://doi.org/10.1016/j.scitotenv.2021.151739.

Yan, J., Zhao, Z., Xia, M., Chen, S., Wan, X., He, A., Daniel Sheng, G., Wang, X., Qian, Q., Wang, H., 2022. Induction of lipid metabolism dysfunction, oxidative stress and inflammation response by tris(1-chloro-2-propyl)phosphate in larval/adult zebrafish. Environ. Int. 160, 107081 https://doi.org/10.1016/j.envint.2022.107081.

Yin, J., Jian, Z., Zhu, G., Yu, X., Pu, Y., Yin, L., Wang, D., Bu, Y., Liu, R., 2021. Male reproductive toxicity involved in spermatogenesis induced by perfluorooctane sulfonate and perfluorooctanoic acid in Caenorhabditis elegans. Environ. Sci. Pollut. Res. Int. 28, 1443–1453. https://doi.org/10.1007/s11356-020-10530-8.

Yoganantharjah, P., Byreddy, A.R., Fraher, D., Puri, M., Gibert, Y., 2017. Rapid quantification of neutral lipids and triglycerides during zebrafish embryogenesis. Int. J. Dev. Biol. 61, 105–111. https://doi.org/10.1387/ijdb.160209yg.

Yu, Q., Huo, J., Zhang, Y., Liu, K., Cai, Y., Xiang, T., Jiang, Z., Zhang, L., 2020. Tamoxifen-induced hepatotoxicity via lipid accumulation and inflammation in zebrafish. Chemosphere 239, 124705. https://doi.org/10.1016/j.chemosphere.2019.124705.

Zhang, Q., Cheng, J., Xin, Q., 2015. Effects of tetracycline on developmental toxicity and molecular responses in zebrafish (Danio rerio) embryos. Ecotoxicology 24, 707–719. https://doi.org/10.1007/s10646-015-1417-9.

Zhang, W., Sheng, N., Wang, M., Zhang, H., Dai, J., 2016. Zebrafish reproductive toxicity induced by chronic perfluorononanoate exposure. Aquat. Toxicol. 175, 269–276. https://doi.org/10.1016/j.aquatox.2016.04.005.

Zhang, Y., Bulkley, D.P., Xin, Y., Roberts, K.J., Asarnow, D.E., Sharma, A., Myers, B.R., Cho, W., Cheng, Y., Beachy, P.A., 2018. Structural basis for cholesterol transport-like activity of the hedgehog receptor patched. Cell 175, 1352–1364.e14. https://doi.org/10.1016/j.cell.2018.10.026.

Zhang, J., Qian, L., Teng, M., Mu, X., Qi, S., Chen, X., Zhou, Y., Cheng, Y., Pang, S., Li, X., Wang, C., 2019. The lipid metabolism alteration of three spirocyclic tetramic acids on zebrafish (Danio rerio) embryos. Environ. Pollut. 248, 715–725. https://doi.org/10.1016/j.envpol.2019.02.035.

Zheng, X.-M., Liu, H.-L., Shi, W., Wei, S., Giesy, J.P., Yu, H.-X., 2012. Effects of perfluorinated compounds on development of zebrafish embryos. Environ. Sci. Pollut. Res. 19, 2498–2505. https://doi.org/10.1007/s11356-012-0977-y.